MAPPING TECHNIQUE BASED ON ELECTRICAL MEASUREMENTS FOR MONITORING THE INTEGRITY OF COMPOSITE PATCH REPAIR IN AERONAUTICAL STRUCTURES

A. Baltopoulos[a], A. Vavouliotis[a], V. Kostopoulos[a*]

[a]*Applied Mechanics Laboratory, Department of Mechanical Engineering and Aeronautics, University of Patras, GR26504, Greece*
**kostopoulos@mech.upatras.gr*

Keywords: composite patch repair, monitoring, electrical sensing, mapping.

Abstract

A technique was formulated and applied to map 1D distributed electrical resistance measurements to a damage inspection 2D map. The exploitation of electrical resistance measurements was based on a probabilistic formulation originating from the field of elastic wave SHM. Appropriate calibration factors were introduced to remove any bias and balance the inspection maps. The damage inspection map provides a distribution (x,y) of probability of damage which is subsequently related to damage presence. The technique was applied to a composite patch repair of an aeronautical aluminium component. The component was subject to fatigue bending loads and IR thermography was used as the benchmarking NDI technique. Recorded results showed that ERCM is sensitive to electrical changed due to debonding of the patch. The mapping technique performed well giving high damage probability in debonded regions. Results were correlated to IR thermography findings and visual inspection.

1. Introduction

The scope of this work is to formulate, establish, implement and assess the performance of an electrical monitoring approach for monitoring the structural integrity of a composite patch repair on a real aeronautical structure. The structural component is the vertical tail stabilizer of an AgustaWestland SW4 helicopter. The part is shown in Figure 1 assembled in the final helicopter, in separate form (for scaling purposes) along with the stabilizer design, patch repair design and implemented composite patch repair. This work was performed in close collaboration with industrial partners from EU-FP7-AAT-IAPETUS project and more specifically from PZL-SWIDNIK who provided the part, the design and implementation of the damage and repair scenario and University of Ioannina for providing the thermography recordings.

The vertical stabilizer is a sandwich composite structure made of aluminum skins and aluminum honeycomb. The part is held in position by 4 bolts at the middle of the part as shown in the schematic (Figure 1). Inserts are used to provide the attachment and tightening points for the bolts. Artificial damage is introduced in the form of a crack close the upper left bolt (Figure 1 bottom left). The definition of this damage case was derived based on experience from in service performance; cracks were usually reported close to the upper right bolt as shown in the picture. The repair scenario is that the crack is at the center of the patch zone. Industrial repair procedures are followed to apply the composite patch. Layers of carbon fabric were pre-impregnated using an epoxy suitable for bonding reinforced with 1%wt MWCNT and then cut to the required dimensions to deliver the layup. When the repair has finished and the patch has cured, the patch is machined to add the insert and pass the bolt through.

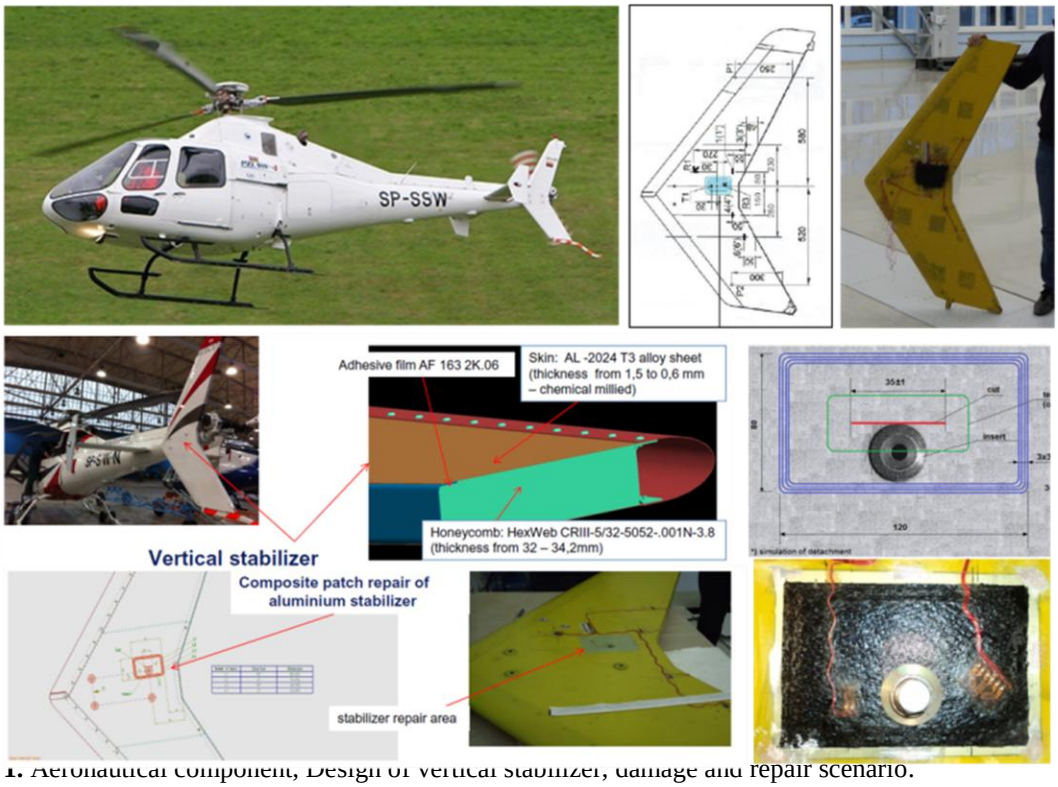

Figure 1. Aeronautical component, Design of vertical stabilizer, damage and repair scenario.

NDI of patch repairs is a very usual procedure in aeronautics these days. Thermal camera imaging is an effective technique [1] for the evaluation of composite repairs both on specimen level as well as component level. Emerging technologies in this direction involve the use of surface acoustic waves [2] and resistive heating in combination with thermal imaging [3, 4] even assisted by nanotechnology [5]. Strain based patch repair integrity monitoring was demonstrated by Baker et al [6] by using strain gages and expanding the idea to FBGs and acoustic emission. Among the emerging technologies are the electrical based techniques for NDI of composite patches which have been limitedly investigated by [7, 8].

In situ electrical methods offer the potential of a tool for health monitoring of composite structures. However, for real case applications such as aeronautical structures or components at large scales, the electrical based techniques need to be further developed, extended and customized to cover the localization and sizing of the evolved damage, as well as cover the practicality of implementation and effectiveness based on the needs of practice. A number of studies have worked in extending electrical sensing principles to 2D using electrical conductivity mapping [9] and electric potential fields [10] on which [8] was based. Other approaches and relevant studies in the field of composites have also been reported. Swait et al [11] proposed a practical health monitoring system based on ERCM approach (Figure 2a). A series of peripheral electrodes was used and simple electrical resistance recordings were able to sense the change due to BVID damage in certain paths. Takahashi et al [12] proposed the deployment of an extensive electrode network over the two sides of a composite panel. The two sets of electrodes are perpendicular (Figure 2b). Resistance recordings through thickness between intersecting electrodes provided a distributed measurement of electrodes. The result is a distributed ERCM over the composites surface. The induced damage is correlated to large drop in electrical resistance. A similar approach was used by Wicks et al [13].

Borrowing principles from Lamb waves [14], Ye et al [15] applied a tomographic approach for quantifying impact damage in composites. The approach establishes distributed sensing paths by creating pairs of electrodes. For each pair a resistance measurement is taken. These are then combined based on weight factors related to spatial distribution and ERCM to deliver the damage probability map (Figure 2c). Here, we follow an approach based on Ye et al [15]. We implement and progress the

mapping technique for delivering damage probability inspection maps derived from electrical measurements made in-situ for patch repaired aluminium components.

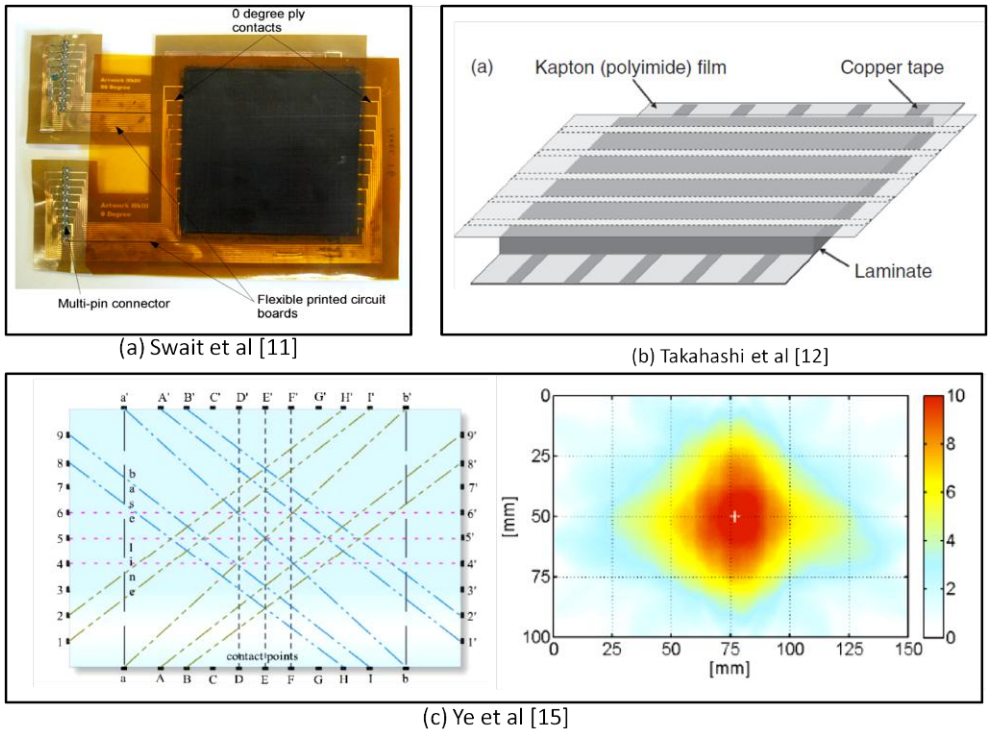

Figure 2. Various electrode arrangements.

2. Electrical monitoring formulation, implementation and experimental approach

2.1. Electrical monitoring technique formulation

The technique established here is based on formerly reported principles and utilizing an adapted post-processing approach provided by Ye et al [15], is targeting in providing a 2D visual evaluation tool for assessing the structural integrity of the composite patch.

The idea for the electrical monitoring formulation is based on the observation reported by Wang et al [16] referred to as current spreading. In principle it is rather intuitive and physically is related to the ratio of the X and Y electrical conductivity of the material in the plane. According to it, when current is injected between two points of e.g. a CFRP plate, the current does not flow in a linear manner. The electric field is diffusive and non-intersecting curved current flow lines are spread in-plane connecting the two points and creating an in-plane potential field. The observation is schematically shown in Figure 3. The electric field E and the respective voltage distribution V developed between points A and B (measurement points) shows the spatial spread in the specimen's plane.

On the practical side of the monitoring technique, most often the quantity in hand is electrical resistance. Usually in field measurements the most easily applied configuration is the 2-point method. To derive the resistance between two points a small current is injected between the points and the voltage is measured. Adding now the current spreading into perspective, the resistance measurement taken is essentially an averaging over the area the current has spread. Thus we shall define a sensing path and a sensing region. We define the sensing path as the straight line connecting the two points of measurement, while the sensing region as the region around the sensing path within which changes are affecting the measurement. We further assume that the closer damage is to the sensing path the higher the influence to the resistance measurement. Thus the sensing region is a weighted region formed around the sensing path. We assume that any change outside this region cannot influence the resistance of this sensing path and is neglected. The sensing region can be calibrated based on a set of

physical parameters. The difference between two measurements taken at different times is required for the technique to work. Any change recorded in the resistance measurement is assumed that is the sole effect of damage within the sensing region.

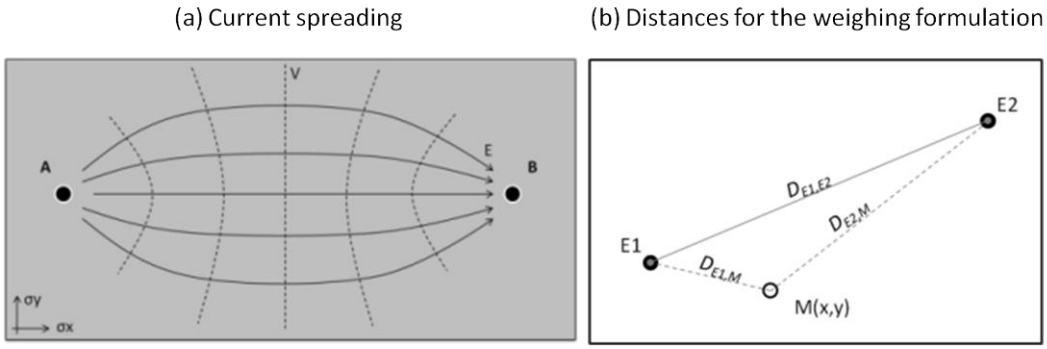

Figure 3. Observation and weight factors

For covering the inspection region (i.e. the patch), an array of electrodes is developed on the periphery of the patch and a central electrode on the patch. The peripheral electrodes are placed on the substrate. The central electrode is co-bonded with the patch during curing. With this arrangement the current injected for the measurement is forced to pass through the interface of the patch and the substrate thus effectively taking into account the integrity of the bond.

The formulation of the post-processing is a modified version of the technique described by Ye et al [14] borrowed from the field of Lamb wave damage detection. Let us assume that there are N pairs of electrodes and N corresponding sensing paths. The electrodes for each pair are denoted E1 and E2. The sensitivity (ΔR/R0) of each sensing path to damage at a specific point M(x,y) depends on the relative position of the point to the active electrodes. To express this dependency, we formulate a relation based on the relative positions of the point to the electrodes of the sensing path. The geometry of the topology is illustrated in Figure 3.

$$R_{SP} = \frac{D_{E1,M} + D_{E2,M}}{D_{E1,E2}} - 1 \tag{1}$$

Where, Di,j – denotes the distance between points i and j. E1 and E2 are the active electrodes for the specific sensing path (SP) evaluated. M is a point on the grid with coordinates (x,y). RSP is calculated for all points on the formed grid forming essentially a weight map over the inspected area. It is a function of (x,y) and it is related to the point M(x,y). Based on this formulation, the weight/influence of a point M is expected to decrease with the increase of the relative position of the point to the SP. The weight has a maximum value of 1 when M falls on the SP. Following the assumption that from a certain distance and on any damage will not affect the measurement, we define a parameter β which essentially sets the weight of the points outside the sensing region equal to zero. This is expressed as follows:

$$W_{SP}(x,y) = \begin{cases} 1 - \frac{R_{SP}(x,y)}{\beta}, & R_{SP}(x,y) \le \beta \\ 0 \quad , & R_{SP}(x,y) \ge \beta \end{cases} \tag{2}$$

The parameter β is selected in such a way so that the sensing regions have the least possible overlap. The behaviour of this parameter is shown later on the application. This relation is of the simplest linear form. Other formulations are possible.

Having these as a basis, the probability (p) of damage being present within the sensing region of a SP is the product of the measurement change and weight factor (map) and is given by:

$$p_{SP}(x,y) = \left(\frac{\Delta R}{R_0}\right)_{SP} \cdot W_{SP}(x,y) \quad (3)$$

Where, ΔR/R0 is the normalized resistance change recorded between two inspection times. WSP is the spatial weight given to ΔR/R0 and maps ΔR/R0 (a 1D measurement) to 2D, while ΔR/R0 is a measure of the probability of damage existence within this path.

Taking the observations of all the sensing paths into consideration, the probability (P) of damage being present at a position (x,y) of the inspected area can be expressed as the cumulative probability contributed by each sensing path:

$$P(x,y) = \sum_{SP=1}^{N} p_{SP}(x,y) \quad (4)$$

The input of this process is the topological characteristics of the monitoring system (i.e. Ei(x,y)) and the recorded resistance measurements. The result of this process is a map covering the inspected area showing the probability of damage presence over the x-y plane. The region with the highest probability is identified as the center of interest.

2.2. Electrical monitoring implementation

For the case of the composite patch, a set of 8 peripheral and 1 central electrodes was selected. This was decided based on the capacity of the available equipment and the dimensions of the area under inspection. In essence, the issue that needs to be assessed is whether or not the patch has debonded or not and where. Thus interest is brought to the interface between the patch and substrate. Therefore, the use of an electrode on the patch was dictated. The peripheral electrodes were positioned at the corners and centers each side of the patch.

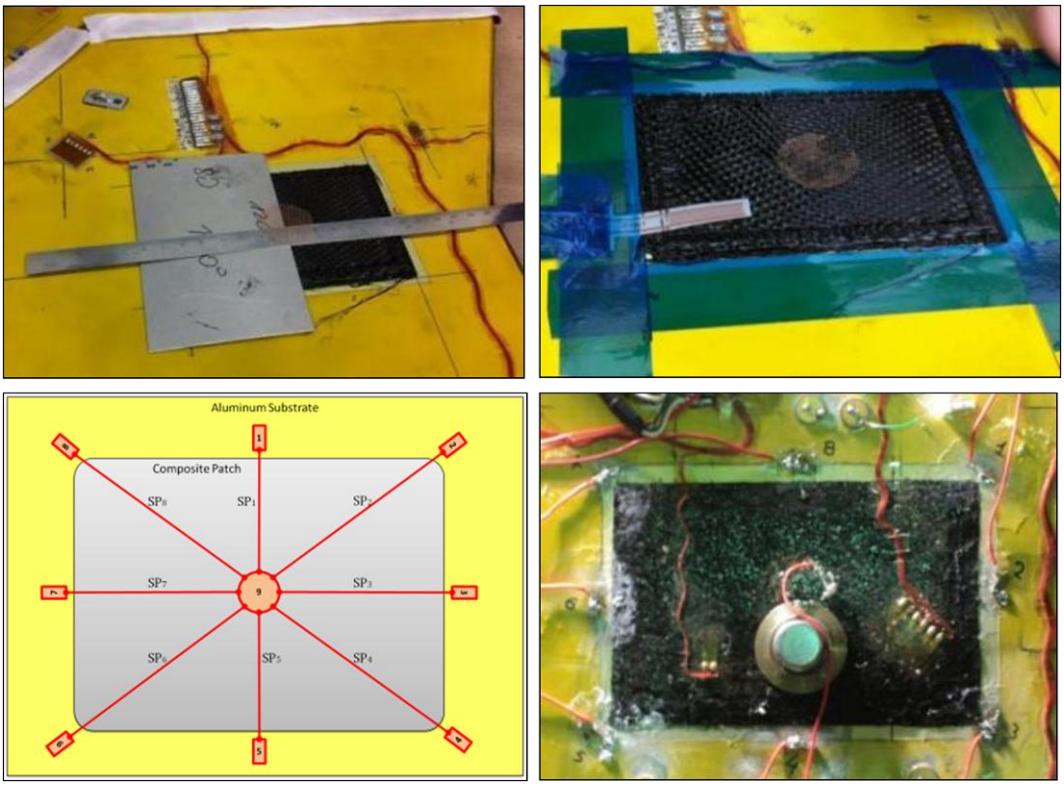

Figure 4. Composite patch repair process, Electrode arrangement and Final setup.

To install the peripheral electrodes at the desired locations a preparation procedure was established. At first the surface of the panel was smoothed out using sandpaper. This was done to remove the paint

and the primer on the aluminium and to get access and contact to the conductive surface. Sanding was continued up to the point when the aluminium was revealed. A small piece (10x20mm) copper mesh was cut and installed by applying cyano-acrylate rapid bonding glue. The glue was cured under pressure using a Teflon film. The copper mesh will serve as the electrode. Then the cured glue was smoothed using sanding paper to reveal the copper mesh. Using standard soldering approaches, cables were then soldered on the copper mesh. For the central electrode, the copper mesh was co-bonded during the application of the patch on the top of the carbon fabric stack. Instances of the procedure are seen in Figure 4 top. Once the patch was cured, the same approach as previously described was followed (i.e. sanding and soldering). The sensing paths resulting from the selected topology are shown in Figure 4 bottom left. The final arrangement of the electrodes on the stabilizer is shown in Figure 4 bottom right.

By taking measurements of the resistance between pairs of points on the patch and the substrate, we get a quantification of the "difficulty" the electrical current faces to pass through this path; the higher the electrical resistance the higher the damage concentration in the path. Thus assuming a direct relation between resistance and damage present in the path we can monitor the changes in the paths resistance and identify the presence of damage. The patch, the bonding adhesive and the substrate are conductive. Therefore any change in the three parts and their respective interfaces will have an effect on the overall electrical measurement. The weakest and most probable parameter for influence is considered to be the interface of the adhesive and the reinforcing phase of the patch (CF) with the substrate.

2.3. Experimental setup

The experimental setup is shown in Figure 5.

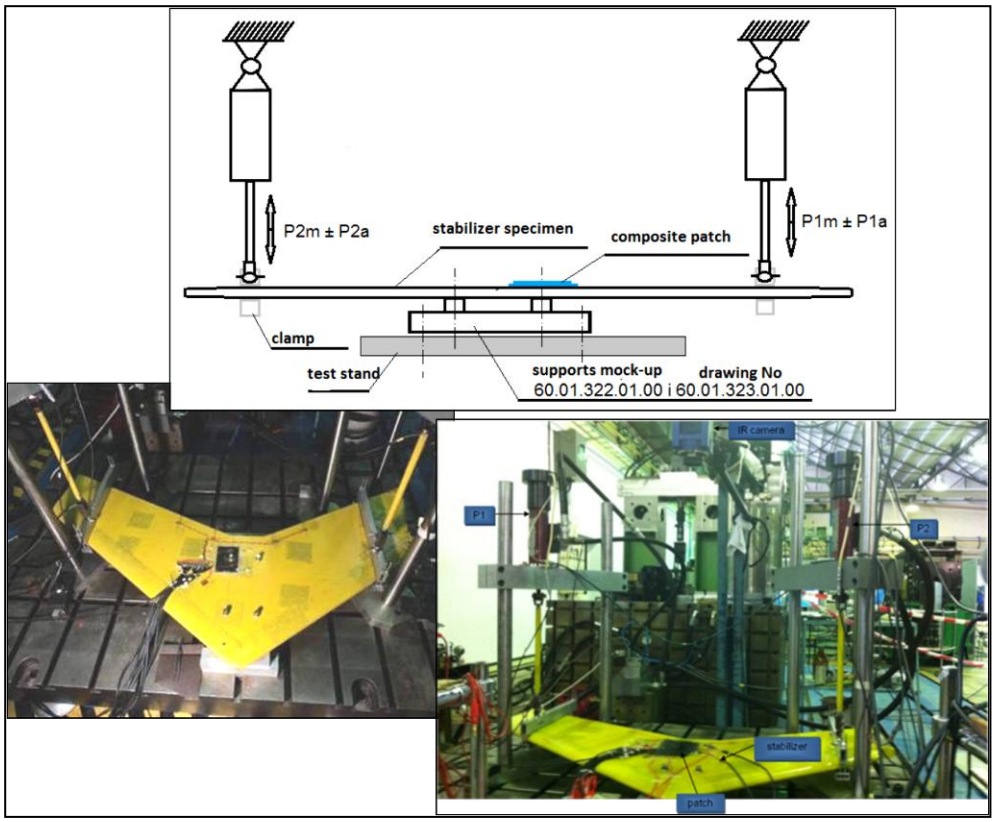

Figure 5. Test setup arrangement.

In service, the vertical stabilizer is held in place by the four bolts. The stabilizer is essentially like a beam clamped at the middle and loaded in bending. During the course of flight the tail rotor is

working, thus producing air pressure on the free surfaces. This is the external loading to the stabilizer. The nature of this load is rather stochastic and due to the prolonged service time the loads can be simulated by fatigue load profiles. To simulate this loading and boundary conditions the following test setup was implemented (see Figure 5). The stabilizer is tightly attached through the bolts on the test bed. The patched side is on top. Two hydraulic pistons are used for controlled external loading, one on each side. The adaptor between the pistons and the device under test (DUT) holds the DUT both on the top and bottom side. The attachment points of the adaptors are not equally distant from the fixation point on the test bed.

Loading was performed in a stepwise manner. The mean value of the loads was kept constant and the amplitude was increasing. The frequency of the load was kept constant at 20Hz. As an average, intervals of 50kCycles were allowed up to 550kCycles. Electrical data acquisition is done in an offline manner by taking resistance measurements between the central and all peripheral electrodes (eight resistance measurements in total). Measurements were performed prior to testing and at certain intervals of fatigue cycles (step). After each step the test was paused and electrical measurements were recorded. Throughout testing, thermography was used as a benchmark technique to monitor damage development and evolution. The configuration is shown in Figure 5 bottom. The IR camera was overlooking the patch region.

3. Results and Discussions

3.1. Calibration of the technique

Once the repair was finished and the electrodes were attached in place, the exact position of the electrodes was defined using image processing software (ImageJ). The respective coordinates were extracted and used for post-processing. The sensing paths are indicated by two digits: SPXY (e.g. SP92). Essentially, β parameter of Equation 2 controls the spread of the sensing region contributing to the measurement. From an alternative perspective, it controls the cut-off point after which no contribution is considered. Each set of electrodes covers a fraction of the inspection area thus producing a weighted sub-map based on the change of the 1D resistance measurements. Due to the use of a common electrode for all the sensing paths the region around the central electrode receives the highest probability. Unit change is used as input for all the SPs. Ideally the sum of all maps should provide a uniform weight maps throughout the inspection region. Therefore an additional calibration factor (Zone Center Factor – ZCF) is introduced to the process that would move the centre of the sensing zone closer to the peripheral electrodes and thus suppress the overlap of the regions.

$$R_{SP} = \frac{ZCF \cdot D_{E1,M} + D_{E2,M}}{D_{E1,E2}} - 1 \tag{8-5}$$

Sensing path	Parameter β	ZCF
91	0.70	1.8
92	1.00	
93	0.70	
94	1.10	
95	0.50	
96	1.00	
97	0.50	
98	1.15	

Table 1. Sensing regions' parameters.

The effect of ZCF is shown in the following Table. Parameters β and ZCF can be selected for each SP to reach a more uniform weight map to be used in the post-processing of the experimental measurements. This will ensure that there is no bias in the estimations. For the specific case study, the parameters were defined are given in Table 1. Practically what is targeted with this parameter

optimization is to reach the maximum sensitivity at the regions close to the edges of the patch. Meanwhile the central region should be kept low to avoid any bias due to the overlapping of the base weight maps. Thus, for the sensing paths having shorter length a larger β parameter is used and for the diagonal sensing paths a much lower value is given. The ZCF factor was kept equal to 1.8 for all the sensing paths. Nevertheless, further customization can be performed to homogenize the sensing region.

3.2 Experimental and post-processing results

During the loading of the structure, the patch is loaded in plane. During fatigue loading the patch starts to debond progressively. The debonding interrupts the conduction paths present either through direct contact of carbon fibres with the aluminium substrate or the bonding between the conductive resin and the substrate. Due to debonding current has limited cross-section to pass through and thus resistance essentially increases. Therefore by recording the resistance for different paths we attempt to follow the initiation and propagation of damage and identify regions of increased damage probability.

Electrical resistance measurements were recorded during the experimental campaign. The measurements were all at the same range of resistance; 0.55-0.85Ω. It is more informative to express the measurements using the relative change of the measurements with respect to a fixed reference point. This is shown in Figure 6. All measurements exhibited a relatively stable behaviour throughout the fatigue test of the stabilizer. At the initial stage a slight drop is exhibited and after 50kCycles the recordings are stabilized. Previous studies on CFRP composite [17] have shown that electrical measurements during fatigue exhibit a drop during the initial stages of loading. Similar behavior were seen here. This is attributed to the fact that after the initial cycles at low loads the system rearranges locally (e.g. electrical connections and contacts, the microstructure of the fibres and the adhesive) and reaches a stable position. At this level no damage is expected. A very small slope is seen for some channels up till 280kCycles. After 280kCycles some channels start to depart from the horizontal indicating a cumulative increase in resistance. This is even more evident at the final stages of the experiment until the final stop. The reference for normalization is taken after the initial drop (@50kCycles). After 280-300kCycles, Channel 3 exhibits a steep increase while all the other channels also show slight increase. At the 50kCycles of the test most of the channels have already a consistent change ~2%, while channels 3 and 4 have exceeded 15% change.

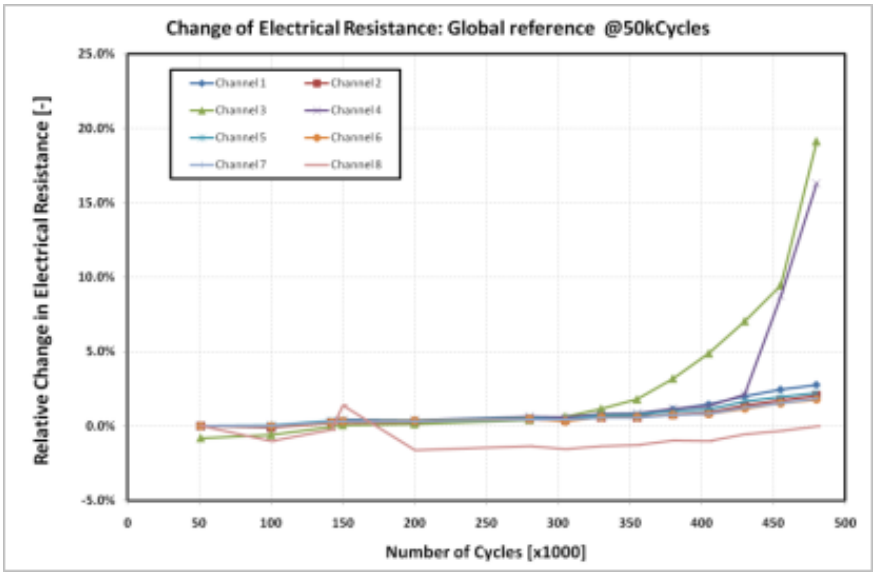

Figure 6. Relative electrical resistance change with reference value at 50kCycles.

A question that usually comes in electrical based damage monitoring is: "How can we be sure that the finding is the one described and not electrode degradation?". Electrode degradation is usually

identified through a couple of indications in the recordings. Firstly, in the case of electrode degradation the recordings are not stable and on every measurement the recordings fluctuate without giving any clear indication. Secondly the changes recorded are usually much larger than the ones exhibited here. As a matter of fact in a failed electrode the term that fluctuates is contact resistance between the electrode and the substrate. In such a case, in a fatigue experiment as the one performed here the variation would be very large and not as consistent as the ones shown in Figure 6. It could be that the central electrode which is common to all sensing paths degrades. However this is highly unlikely as firstly the central electrode is co-bonded during the curing of the patch and secondly the attachment of the peripheral electrodes is much weaker. In addition, the amplitude values of strains during the test are presented in Figure 7. The strain gauges were located throughout the components surface and close to the patch location.

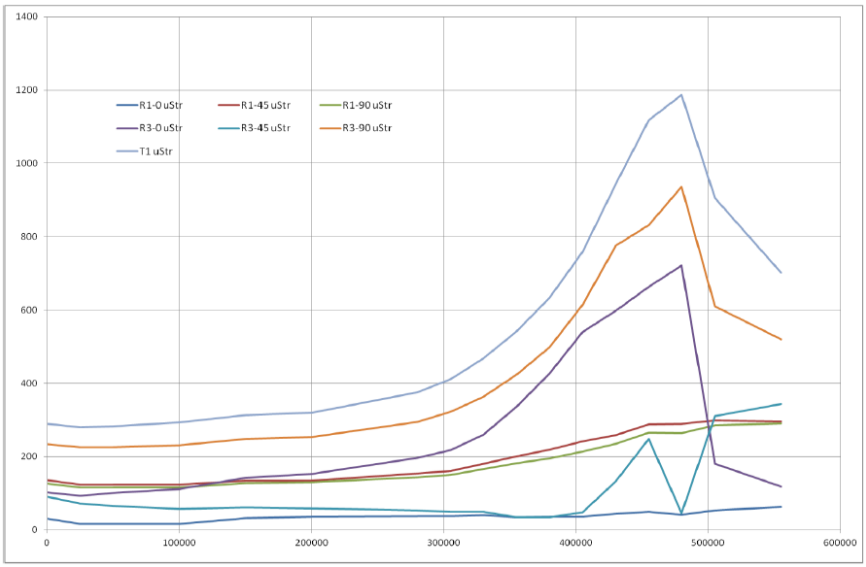

Figure 7. Amplitudes of strains obtained during fatigue testing.

The recorded 1D measurements are then processed following the described algorithm to deliver the damage probability maps for inspecting the integrity of the composite patch. A series of maps was calculated for different states (after a number of certain kCycles). A selection of these maps is shown in Figure 8.

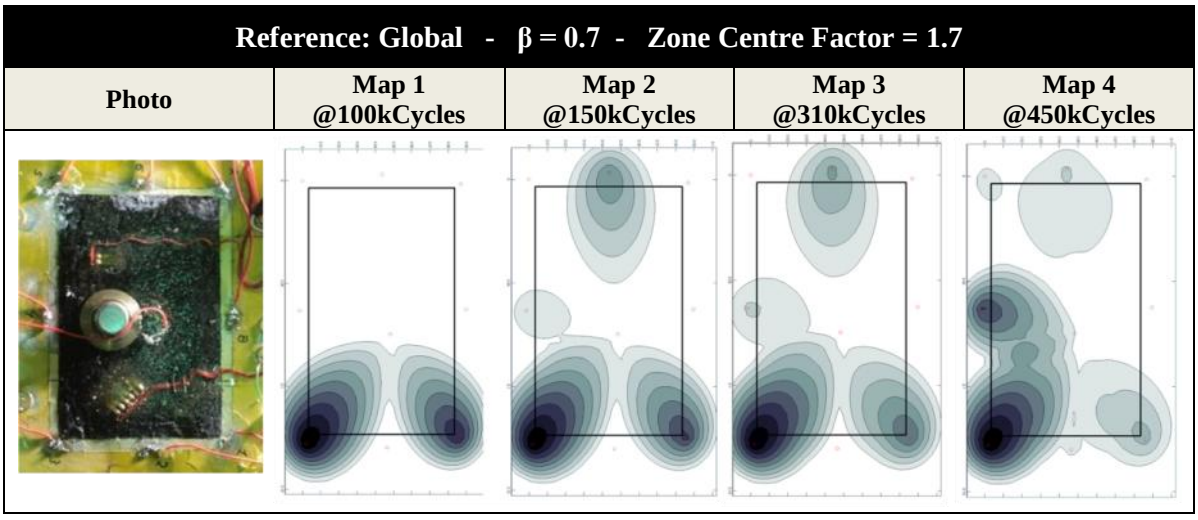

Figure 8. Damage probability maps for composite patch repair based on electrical resistance measurements.

Starting from the left, a photo of monitored system is presented followed by four damage probability maps. The first map is calculated for the state at 100kCylce. This is after 50kCycles from the

reference. The map shows an increased damage probability on sensing regions 1 and 3. Due to the high relative resistance change recorded, sensing path 3 exhibits a higher probability. After 50kCycles, the map shows multiple regions of interest. The region previously identified gives indications of propagation towards sensing region 4. An additional region is identified at sensing region 6. The same trend is seen further at 310kCycles (after 160kCycles) with an increase in sensing region 4 and a slight increase in 1 and 3. Sensing region 6 remains relatively unchanged. Finally, in map 4, interest has evidently shifted to sensing regions 3 and 4 with very high probability while the previously indicated regions have been shadowed by the dramatic increase in regions 3 and 4.

To verify the findings of the electrical mapping technique proposed in this work, data recorded using thermographic imaging are used. More specifically lock-in thermography data are presented in Figure 9. The advantage of lock-in thermography is the fact that one can get both amplitude and phase information. At the top is the amplitude image and at the bottom is the phase image. In the first two phase images the artificial crack is evident through the patch.

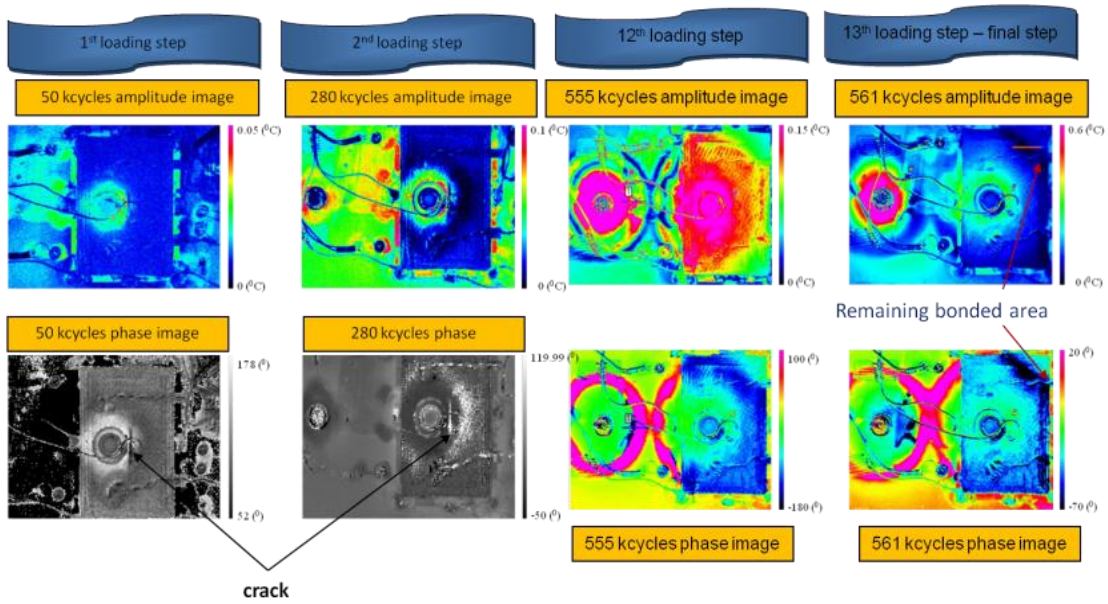

Figure 9. Lock-in thermography recordings [18].

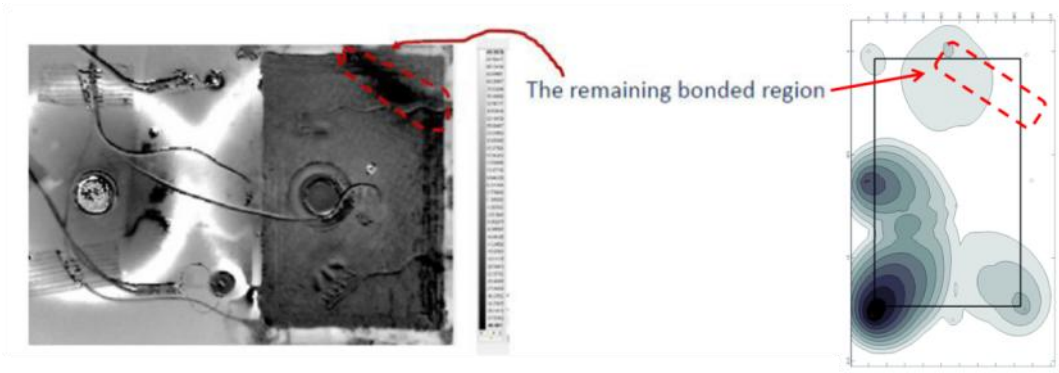

Figure 13. Thermography Vs. Damage probability map based on electrical resistance recordings.

In Figure 13 a direct comparison between the result of the proposed and the benchmarking technique is attempted. After some cycles the patch has debonded almost completely apart from a small region at the top right corner of the patch as viewed. The boundary of this region is seen in the thermography image as a darker region and is indicated in red. The same region is projected onto the electrical mapping result. It is seen that the damage probability map has successfully indicated that the lower regions of the patch are more probable to have been debonded. Interestingly, sensing region 8 hasn't given any indication of debonding even though the patch has lost its integrity. Revisiting the relative

resistance change recordings, it is evident that due to the reference the recording for this channel remain lower than the rest of the channels. A correction may be done here but this would bias the outcome.

4. Conclusions

A practical mapping approach for patch repair monitoring utilizing distributed electrical resistance measurements has been formulated and experimentally verified on a real aeronautical part under simulated service conditions loading. The inputs of the technique are the topological characteristics of the monitoring system (i.e. coordinated of the electrodes Ei(x,y)), the measurement pairs and the recorded resistance measurements.

During fatigue loading the patch starts to debond progressively. Debonding interrupts the conduction paths present either through direct contact of carbon fibres with the aluminium substrate or the bonding between the conductive resin and the substrate. Due to debonding resistance is expected to increase. This was verified experimentally. When a change is recorded in a measurement, it can be translated in that a change is present within the sensing region of the specific measurement. By establishing a distributed set of sensing pairs a whole region can be covered. Having multiple sets of measurements this can lead to a spatial representation of the damage probability. Through a formulation which is assuming sensing regions and weighing factors to cover the inspection area, the result of this process is a damage probability distribution map covering the inspected area showing the probability of damage presence over the x-y plane. The technique serves as a tool for translating a set of 1D resistance measurements into 2D maps taking into consideration the spatial distribution of the sensing points and the influence region of each measurement. The findings of the technique were verified against thermal imaging techniques.

From these observations and results, it is seen that electrical recordings have provided important information and with the assistance of the proposed mapping technique the information is further visualized and better assessed. The proposed methodology has a simple formulation and thus a lot of space is available for improvement given the effective monitoring demonstrated through this work.

Acknowledgements

This work has been funded under the framework of the EU-FP7-AAT project IAPETUS (Grant Agreement Number: ACP8-GA-2009-234333).

References

[1] Paipetis et al. In Service Damage Assessment of Bonded Composite Repairs with Full Field Thermographic Techniques, Proc. of the SPIE Conference on Nondestructive Characterization for Composite Materials, Aerospace Engineering, Civil Infrastructure, and Homeland Security, vol. 7983, Article Number 79831U, DOI: 10.1117/12.880376, (SPIE - The International Society for Optical Engineering, San Diego, CA, 2011).

[2] Sofia Pavlopoulou et al. Structural Health Monitoring of Composite Scarf Repairs with Guided Waves, 2012, Key Engineering Materials, 518, 328

[3] Athanasopoulos et al. Damage detection via Joule effect for multidirectional carbon fiber reinforced composites. Appl Phys Lett 2012;101(11): 114109-114109-5.

[4] Ahmed et al. Heat emitting layers for enhancing NDE of composite structures. Composites Part A: Applied Science and Manufacturing, 39(6):1025-1036, 2008.

[5] Guzman de Villoria et al. Multi-physics damage sensing in nano-engineered structural composites. Nanotechnology 2011;22:185502.

[6] Baker et al. Towards a practical structural health monitoring technology for patched cracks in aircraft structure. Composites: Part A 40 (2009) 1340–1352

[7] Vavouliotis, et al. On line monitoring of damage during fatigue loading of composite patch repair of composite structures, 2012, Emerging Technologies in Non-Destructive Testing V - Proceedings of the 5th Conference on Emerging Technologies in NDT , pp. 395-399

[8] Ampatzoglou, A., Vavouliotis, A., Baltopoulos, A., Kostopoulos, V. Non destructive evaluation of artificially induced damage in composite structures using electrical resistance/potential

mapping. 2012, Emerging Technologies in Non-Destructive Testing V - Proceedings of the 5th Conference on Emerging Technologies in NDT , pp. 381-387

[9] Schueler et al. Damage detection in CFRP by electrical conductivity mapping. Compos Sci Technol 2001;61:921–30.

[10] Angelidis et al. Detection of impact damage in CFRP laminates by means of electrical potential techniques. Comp Sci Technol 2007;67:594–604.

[11] Swait et al. A practical structural health monitoring system for carbon fibre reinforced composite based on electrical resistance. Composites Science and Technology, Volume 72, Pages 1515–1523, 2012.

[12] Takahashi et al. Towards practical application of electrical resistance change measurement for damage monitoring using an addressable conducting network. Structural Health Monitoring 2012;11(3):367–377.

[13] Wicks et al. Health Monitoring or Carbon NanoTube (CNT) Hybrid Advanced Composite for Space Applications. Proceedings of the 11th European Conference on Spacecraft Structures, Materials and Mechanical Testing, Toulouse, France, September 2009.

[14] Wang et al. A Probabilistic Diagnostic Algorithm for Identification of Multiple Notches Using Digital Damage Fingerprints (DDFs), Journal of Intelligent Material Systems and Structures 2009 20: 1439

[15] Ye et al. Interlaminar fracture and impact damage assessment by electrical resistivity tomography in GFRP laminates with conductive nanoparticles. Proceedings of the ECCM15 – 15th European Conference on Composite Materials, Venice, Italy, 24-28 June 2012.

[16] Wang et al. Sensitivity of the two-dimensional electric potential/resistance method for damage monitoring in carbon fiber polymer-matrix composite. J Mater Sci 2006; 41:4839–4846.

[17] Vavouliotis et al. On the fatigue life prediction of CFRP laminates using the Electrical Resistance Change method. Composites Science and Technology 71 (2011) 630–642

[18] Grammatikos S.A. Structural integrity assessment of aerostructures using innovative Non-Destructive Evaluation Techniques. PhD Thesis, University of Ioannina, Greece (2013)